

1 **Experimental study on effective utilization of industrial solid wastes in developing Ultra-High**
2 **Performance Geopolymer Concrete**

3

4 M Sathyanarayanan¹, D Brindha²

5 ¹Thiagarajar College of Engineering, Madurai, Tamil Nadu, India.

6 ² Thiagarajar College of Engineering, Madurai, Tamil Nadu, India.

7 *Corresponding author: M Sathyanarayanan

8 E-mail: sathya15289@gmail.com, tel: 9994548417

9

10

11

12

13

14

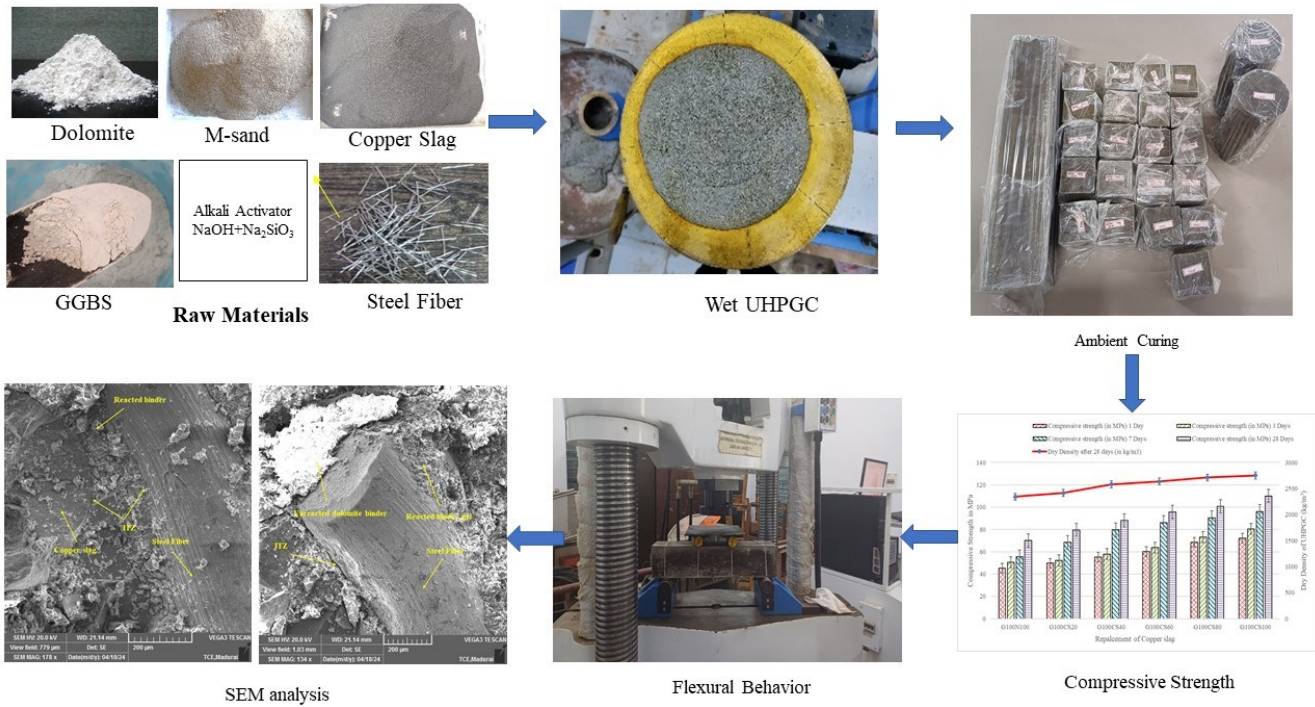
15

16

17

18

19 **Graphical abstract:**



20

21 **Abstract:**

22 This experimental study explores the use of Ground Granulated Blast Furnace Slag(GGBS) and dolomite
 23 as alkali activated binders and copper slag as aggregate to achieve a cost-effective and sustainable Ultra-
 24 High-Performance Geopolymer Concrete(UHPGC). Several concrete compositions utilizing copper slag
 25 as a substitute for natural aggregates were formulated. Tests have shown that the inclusion of 100%
 26 copper slag fine aggregate leads to significant improvements in the mechanical properties and density of
 27 geopolymer concrete. Specifically, the compressive strength increased by 56.8% and the density
 28 increased by 17.5%. To understand the influence of dolomite in GGBS binder, several mixes varying
 29 dolomite proportion in GGBS were examined. The compressive strength of the 80% GGBS/20%
 30 dolomite geopolymer matrix is 32.8% higher compared to the compressive strength of UHPGC
 31 with 100% GGBS. The UHPGC mixture containing 1% crimped steel fibers showed the highest
 32 compressive strength, measuring 146.6 MPa. The split tensile and flexural strengths of the 20% dolomite

33 matrix show a significant increase of 30.55% and 30.24% respectively compared to the 100% GGBS
34 matrix. The water absorption and porosity of the 100% GGBS specimen were found to be lower
35 compared to the 20% dolomite UHPGC specimen. The microscopic study reveals the positive impact of
36 dolomite and GGBS on enhancing the bonding of the geopolymer matrix along with decreasing
37 permeability. This study highlights the potential of geopolymer technology in producing ultra-high-
38 performance concrete using GGBS, dolomite, and copper slag.

39 **Keywords:** Geopolymer concrete, GGBS, Dolomite, Copper slag, Fine aggregate, Mechanical
40 properties, Durability, Sustainable construction.

41 **1. Introduction**

42 Ultra-High-Performance Concrete (UHPC) is an emerging construction composite with superior
43 compressive strength (typically greater than 120 MPa), high flexural strength, remarkable toughness, and
44 durability requirements (X.-H. Wang et al., 2017; Yoo et al., 2016). These outstanding performances are
45 made possible through rapid mixing, peculiar proportioning and special curing techniques. The important
46 aspect in developing UHPC is the heavy consumption of Portland Cement (PC). UHPC contains typically
47 850 to 1200 kg/m³ of PC which is thrice the quantity required for conventional concrete. As a result,
48 UHPC's extensive use is limited because to its high energy consumption and ensuing rise in materials
49 cost (Habert et al., 2013). Research has been made to find a suitable alternate binding material for PC-
50 based binding system. Utilizing Supplementary Cementitious Materials (SCM) derived from industrial
51 leftovers such as metakaolin, fly ash, ground granulated blast furnace slag (GGBS), Alccofine, and Rice
52 Husk Ash (RHA) as a partial substitute for PC in UHPC offers a methodical strategy that effectively
53 minimizes trash accumulation in landfills (Kavitha and Felix Kala, 2016; Sharma and Sivapullaiah, 2016;
54 R and J, 2019; Ansari and Bandewar, 2022).

55 Geopolymer binders, are the clinker free binders utilizing 100% SCM which achieves comparable
56 mechanical properties and superior durability properties(Singh et al., 2015; Sontakki and Cholekar, 2015;
57 de Oliveira et al., 2022; Wong, 2022). Geopolymer Concrete (GPC) is produced when aluminosilicate
58 minerals dissolve in the alkaline activation solution and repeatedly interact with Si–O–Al–O in an
59 amorphous state. Joseph Davidovits developed three distinct varieties of geopolymers on the basis of the
60 various shapes of chemical bonds that result from hydrothermal processes. It includes sialates (-Si-O-Al-
61), poly sialate (-Si-O-Al-O-)n, and poly-sialate siloxo (-Si-O-Al-O-Si-O-)n. (Davidovits, 1991). Being
62 the most common and affordable aluminosilicate source, the low calcium flyash based geopolymer
63 binders require heat curing for the polymerization process which makes the GPC technology less feasible
64 in construction industry(Hardjito et al., 2005; Yunsheng and Wei, 2006). “Several attempts have been made
65 to explore the potential of using solid crushed wastes such as recycled concrete waste powder and waste
66 clay brick powder as alternative precursors for geopolymer binder. Huixia Wu et. al explored the use of
67 recycled concrete powder (RCP) and recycled paste powder (RPP) in their study on high-ductility
68 Engineered Geopolymer Composites (EGC) and UHPC(Wu, C. Liu, et al., 2024; Wu, X. Liu, et al., 2024).
69 The clay brick waste, commonly used for filling, has proven to be a highly effective precursor for alkali
70 activated composites(Wu, Gao, et al., 2024). At present, scholarly attention is focused on exploring the
71 development of geopolymer concrete in ambient conditions as a way to reduce curing energy demands
72 and enable the technology to be implemented for in-situ concreting. Despite the fact that numerous
73 alternative SCMs can enhance their strength during elevated curing, ambient cured geopolymer concrete
74 can be formulated only by using GGBS as the primary binder. (Patil, Karikatti and Chitawadagi, 2018; Amar
75 et al., 2023; Chithambar Ganesh et al., 2023).

76 The GGBS is a by-product resulted from the molten iron in the smelting process of iron ore. Being the
77 second largest by-product produced in India after flyash, GGBS is mainly utilized as a partial replacement
78 of cement in the conventional concrete(Sharma and Sivapullaiah, 2016). It was reported that the quantity

79 of GGBS dissolved is greater than that of fly ash dissolved in a geopolymer medium(Panagiotopoulou et
80 al., 2007). It is generally observed that the compressive strength of geopolymer concrete tends to increase
81 with higher slag content. The limited dissociation of the glass phase in fly ash results in a minimal
82 production of C-(A)-S-H. Due to the utilization of GGBS as its primary binder, GPC has garnered
83 considerable interest in recent years on account of its superior chemical and temperature resistance, low
84 permeability, and high initial compressive strength. Studies reveals that Ultra-High Performance
85 Geopolymer Concrete (UHPGC) can be developed by using GGBS and silica fume as binding
86 precursors(Ambily et al., 2014). A.Wetzel et al.(2019) summarized the superior effect of metakaolin and
87 silica fume in GGBS for higher polymerization degree in the reaction products(Wetzel and Middendorf,
88 2019). The study also revealed the possibility of balancing workability and strength parameters. Liu et
89 al. (2020) reports the development of Ultra-High Performance Geopolymer Concrete (UHPGC) using
90 GGBS and overcoming the brittleness feature of geopolymer matrix by using different steel fibers(Ding,
91 Shi and Li, 2018; Liu et al., 2020a). It is widely recognized that augmenting the source material dissolution
92 results in a greater quantity of C-A-S-H gel, thereby enhancing the concrete's mechanical properties.
93 Slag-based geopolymer concrete have practical obstacles, including quick setting (less than 30 minutes),
94 which limits their application in mix-ready and pumped concretes(Dineshkumar and Umarani, 2020).
95 The necessity for novel binders with equivalent strength performance as GGBS arose due to the
96 workability and desired setting time needed for casting concrete. Studies reveal that high strength GPC
97 may be produced from GGBS and dolomite(Saranya, Nagarajan and Shashikala, 2020). The inclusion of
98 dolomite to slag-based GPC increases setting time and workability, and significantly improves early-age
99 strength(Saranya, Nagarajan and Shashikala, 2019).

100 Dolomite is a double carbonate of calcium and magnesium occurring naturally as a sedimentary rock.
101 Dolomite predominantly consists of Calcium carbonate and Magnesium carbonate(Goldsmith and Graf,
102 1958). In 1792, Swiss naturalist Nicolas de Saussure discovered dolomite for the first time and designated

103 it with the specific name "dolomite" in reference to its first describer, Dolimeu. Previous studies reveal
104 that Waste Dolomite Powder (WDP) obtained as the by product from the dolomite rock crushing plant
105 in the process of manufacturing dolomite products can be effectively utilized as precursor, fine aggregate
106 and coarse aggregate in concrete(Hu, Yao and Wei, 2023). When CaCO_3 contributes early strength,
107 MgCO_3 in conventional concrete makes the composites more workable as it dissolves easily than
108 CaCO_3 (Azimi et al., 2020). Similarly, in geopolymer concrete the dolomite reduces the quickness in the
109 reactivity by providing high workability and comfortable setting time even for the lesser liquid binder
110 ratio(Divekar and Sawant, 2023). That may overcome the disadvantage of GGBS based geopolymer
111 composite which starts dehydrate rapidly. Understanding the function of precursors in developing
112 UHPGC, through mechanical behavior and microstructural analysis is the primary aim of this study.

113 Meanwhile, the increasing demand for natural resources such as river sand and crushed aggregate poses
114 a significant threat to the delicate ecological balance. Thus, the depletion of natural resources for building
115 material sector leads to the associated many environmental effects like global warming and loss of bio
116 diversity. The replacement of aggregates by industrial by products is a vast study in the civil engineering
117 research. The ceramic waste, granite waste, copper slag, recycled aggregates and coral aggregates are the
118 few alternate sources that can be replaced partially or completely in natural aggregates for the
119 development of concrete composites (Shi, Meyer and Behnood, 2008; Brindha and Nagan, 2011; Rajasekar,
120 Arunachalam and Kottaisamy, 2018; Iyengar et al., 2019; Wang et al., 2019). Brindha et al. (2011) revealed that
121 replacement of copper slag in PC based concrete increased the self-weight by 20%. The also revealed
122 that addition of copper slag up to 40% showed promising results in mechanical behavior. Many research
123 studies show that copper slag as fine aggregate can also be utilized for UHPC. The compressive strength
124 of 158 MPa was achieved by using copper slag fine aggregate(Ambily et al.,). Copper slag is a by-product
125 that is acquired during the process of matte smelting and refining of copper. Utilizing copper slag offers

126 both environmental and economic benefits. It helps reduce the need for landfill space and meets the
127 growing demand for natural aggregates in the concrete industry(Vinotha Jenifer et al., 2023).

128 A thorough investigation has been conducted to examine the mechanical properties of UHPGC by
129 incorporating varying quantities of copper slag instead of natural crushed aggregates in the phase-I of
130 this study through flowability and compressive strength. Following the optimization of aggregates, the
131 mechanical properties of the UHPGC samples that included dolomite as a partial substitute for GGBS
132 were examined. The use of Scanning Electron Microscopy (SEM) analysis has greatly enhanced the
133 analysis of this experiment at a microscopic level. Therefore, the research aimed to assess the practicality
134 of using GGBS, dolomite, and copper slag in the production of UHPGC, making it more cost-effective
135 for wider application.

136 **2. Experimental program**

137 2.1. Materials

138 2.1.1. Binder

139 The geopolymer binders were prepared by alkali activation of precursors like GGBS and dolomite. The
140 GGBS was procured from JSW cement limited, Maharashtra, with 28 days Slag Activity Index being
141 89.80%. The chemical composition arrived from the XRF fluorescence analysis is displayed in Table 1,
142 which confirms the chemical requirement recommended by IS 16714: 2018(IS 16714, 2018). The
143 dolomite of size 800 US mesh varies from 8μ to 12μ was used as another precursor to optimize the binder
144 materials to achieve better rheological properties. The chemical composition of dolomite as tabulated in
145 Table 1 shows that the material composition is very similar to the GGBS except the content of Alumina
146 and magnesia. The reactive CSH gels formation from the oxides of calcium ensures the uniform strength
147 development by GGBS and dolomite. The GGBS and dolomite are shown in the Figure 1, where it can
148 be seen that the color of GGBS is greyish white and dolomite being pure white in color.



a)

b)

149
150
151 **Figure 1.** a) Ground Granulated Blast Furnace Slag (GGBS) b) Dolomite

152 **Table 1.** Physical and chemical properties of precursors

Oxide Composition (percentage by mass)	GGBS	Dolomite
CaO	37.63	36.32
SiO₂	34.81	19.23
Al₂O₃	17.92	8.24
Fe₂O₃	0.66	2.44
MgO	7.80	21.22
MnO	0.21	0.06
CL	0.004	0.03
SO₃	0.19	-
IR	0.20	0.09
Specific Gravity	2.91	2.86
Blaine's fineness(cm ² /g)	4032	3500
Colour	Greyish white	White

153

154

155

156 2.1.2. Aggregates

157 In order to achieve the ultrahigh strength confirming to ASTM C1856, the maximum aggregates size was
 158 restricted to 1.18 mm to ensure the homogeneity of the concrete(Ambily et al., 2014). The fine aggregates
 159 used in this study were natural crushed aggregates and copper slag of zone II grading confirming IS
 160 383(1970)(Kisan and Sangathan, 1970). The physical properties of natural sand and copper slag are
 161 tabulated in Table 2. Copper slag was brought from Sterlite Industries India Limited, Tuticorin, Tamil
 162 Nadu, India. The copper slag and natural crushed aggregates received from the suppliers were sieved
 163 under 1.18 mm sieve and it was wetted to attain Saturated Surface Dry Condition (SSD) before casting.

164 **Table 2.** Physical properties of natural sand and copper slag

Physical Property	Specific gravity	Bulk Density(g/cm ³)	Water Absorption (%)	Fineness modulus	Mean Size (Range)
Natural Sand	2.603	1.811	4.2	3.21	925 μ
Copper slag	3.570	2.044	0.52	3.74	1.03 mm



166 a)

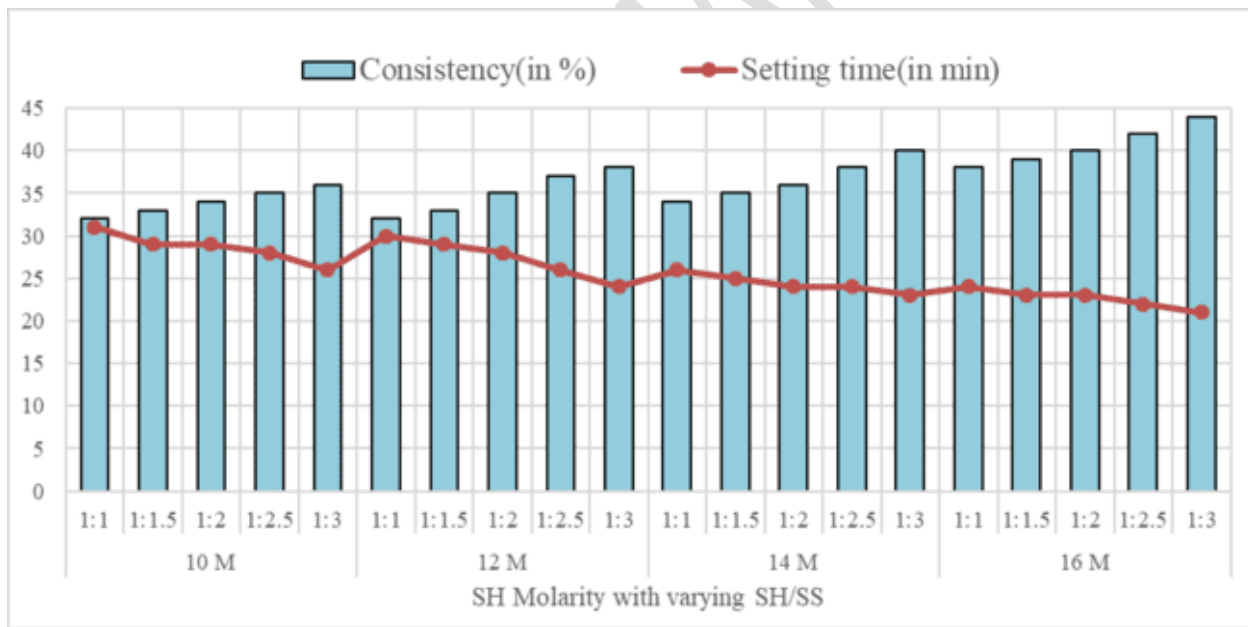
b)

167 **Figure 2.** a) Natural Crushed aggregates(M-Sand) b) Copper Slag

168 2.1.3. Alkali activators

169 The alkali activation of the precursors was done by Sodium Hydroxide (SH) and Sodium Silicate (SS).
 170 The sodium silicate solution's specific gravity was determined to be 1.54. A solution of sodium hydroxide
 171 was prepared by mixing caustic soda pellets with water. The pellets had a high purity level of 97%–98%
 172 and a specific gravity of 1.47. It is evident from the previous research findings that as the ratio of SH and

173 SS and molarity of SH increases, the compressive strength will be increased(Ahmed, Kumar and Nanda,
 174 2021; Chithambar Ganesh et al., 2023). The consistency in Vicat apparatus and Flow table tests confirming
 175 to IS 4031(Part-4) - 1988 and IS 5512 – 1983 were performed to optimize the SH/SS and SH molarity
 176 for comfortable workability and reasonable setting time. The consistency and setting time of various
 177 mixes are illustrated graphically in Figure 3. From these preliminary tests and practical difficulties learnt,
 178 the liquid binder ratio was taken as 0.38, the ratio of Sodium hydroxide and sodium silicate and the
 179 molarity of sodium hydroxide was fixed as 1:2 and 14 M respectively to balance the strength and
 180 workability of the mix. For UHPGC with fibers, the matrix needs to be in a flowable consistency. Hence,
 181 the Polycarboxylate Ether (PCE) based superplasticizers were used to increase the workability without
 182 compromising the strength gain of concrete. The quantity of superplasticizers taken were restricted to
 183 2% by weight of the of the binder.



184
 185 **Figure 3.** Consistency and Setting time vs Alkali activator concentration

186 2.1.4. Steel fibers

187 Micro steel fibers in geopolymer composites enhances the flexural behavior. The micro crimped steel
 188 fibers as shown in the Figure 4 was used in this experiment to enhance the ductile properties to UHPGC.
 189 The steel fibers length in this study was restricted to 20 mm as the longer steel fibers may affect the inter
 190 fiber spacing which may form a network of fibers that leads to weak zone in concrete. The steel fibers of
 191 aspect ratio more than 50 was used. The mechanical behavior, particularly in terms of flexural strength,
 192 is significantly influenced by the deformation ratio (R_D) of the fibers. (Liu et al., 2020a). R_D for round
 193 crimped fibers is 1.33. The properties of steel fiber are listed in Table 3.



194
 195 **Figure 4.** Crimped steel fibers

196 **Table 3.** Properties of steel fiber

Geometry	Density (kg/m^3)	Length (mm)	Diameter (mm)	Aspect ratio (length/diameter)	Tensile strength (MPa)	Deformation ratio
Crimped	7850	20	0.4	50	2820	1.33

197 **2.2. Mix composition**

198 As there are no standard method available for designing the mix proportion for UHPC and UHPGC, from
 199 the trial mixes and literature work the mix composition were derived. In order to make the mix denser
 200 with high packing density, the equal proportion of binder and aggregate were taken. The liquid binder
 201 ratio of 0.38 was maintained for all the mixes. Table 4 provides an overview of the mix composition of
 202 different mixes. A two-phase study was carried out to minimize material waste. In first phase the
 203 optimization of copper slag content in fine aggregate was investigated. The replacement of copper slag

204 with varying percentage to natural aggregates (0-100%) were experimented for concrete compressive
 205 strength. After optimizing the copper slag content, the influence of dolomite as binder in mechanical and
 206 micro properties were studied. The crimped steel fibers by volumetric addition by 1.0 % were added.

207 **Table 4.** Mix composition of various mixes

Mix ID	Binder		Aggregate		Alkali activator		Steel Fibers	SP
	GGBS	Dolomite	NA	CS	NaOH	Na ₂ SiO ₃		
Phase-I (Copper slag Optimization)								
N100	1195	0	1195	0	151.4	302.7	0	24
CS20	1195	0	956	239	151.4	302.7	0	24
CS40	1195	0	717	478	151.4	302.7	0	24
CS60	1195	0	478	717	151.4	302.7	0	24
CS80	1195	0	239	956	151.4	302.7	0	24
CS100	1195	0	0	1195	151.4	302.7	0	24
Phase-II (Dolomite Optimization)								
G100D0SF0	1195	0	0	1195	151.4	302.7	0	24
G100D0SF1	1195	0	0	1195	151.4	302.7	78.5	24
G90D10SF0	1075.5	119.5	0	1195	151.4	302.7	0	24
G90D10SF1	1075.5	119.5	0	1195	151.4	302.7	78.5	24
G80D20SF0	956	239	0	1195	151.4	302.7	0	24
G80D20SF1	956	239	0	1195	151.4	302.7	78.5	24
G70D30SF0	836.5	358.5	0	1195	151.4	302.7	0	24
G70D30SF1	836.5	358.5	0	1195	151.4	302.7	78.5	24
G60D40SF0	717	478	0	1195	151.4	302.7	0	24
G60D40SF1	717	478	0	1195	151.4	302.7	78.5	24

208 NA-Natural Aggregate; CS-Copper Slag; SP-Superplasticizers

209 2.3. Preparation of samples and curing

210 Ensuring the workability of geopolymer concrete is crucial when using alkali activators. To prevent water
 211 absorption from the AAS, it is important to use aggregates in a saturated surface dry condition. The
 212 aggregate is allowed to immerse in the water and dried in room temperature in a large tray, so that there
 213 is no moisture in the surface of the aggregates. Instead of adding additional water during mixing process
 214 to achieve the minimum workability, this process would improve the workability in a healthy way which
 215 leads to the appropriate gel formation resulting better binding between powder material and

216 aggregates(Kathirvel and Sreekumaran, 2021)A 20 L vertical vane type mixer with variable speed control
217 was used for the mixing operation. The dry materials including binder and aggregates in SSD condition
218 were mixed at 200 rpm speed for two minutes. Half of the alkali activating liquid prepared was added to
219 the dry mixture and allowed to mix for another 2 minutes. Now the remaining liquid along with the
220 diluted superplasticizers were added followed by the final mixing for 5 minutes at 450 rpm. The well
221 mixed concrete is transferred to cube, cylinder and prism molds. Mixes with higher concentrations of
222 dolomite and copper slag had a higher setting time and were easier to deal with because of their greater
223 fluidity. The beneficial aspect of mixes with high workability without adding more liquid is that they
224 may enhance the gel's binding capability with aggregates. Wan et al, investigated about the effect of steel
225 fibers dispersion in the flexural strength of the concrete(Wan et al., 2020). The placement method of
226 concrete decides the dispersion of steel fibers and fiber orientation. Concrete was poured in the center of
227 the prism and allowed to spread out along its length by external vibration, as evidenced by earlier research
228 showing that specimens produced by pouring concrete in the center had higher flexural strength. Once
229 the surface is finished, the exposed surface of the cast specimen in mold was covered with wrapping
230 sheet to avoid the rapid expelling of water to atmosphere. After 24 hours of casting the specimen was
231 demolded. It is essential to promptly cover the specimen with a plastic sheet due to the usage of minimal
232 amount of liquid and absence of bleed water in UHPGC. This surface drying can potentially affect the
233 hardened properties.

234 The GGBS based geopolymer concrete does not require special curing regimes like heat curing and steam
235 curing to achieve the desired strength. The high calcium GGBS leads to Calcium Alumina Silicate
236 (CASH) gel in room temperature whereas the low calcium SCM based geopolymer composites (like fly
237 ash, metakaolin and silica fume) requires high temperature curing for polymerization process. Hence all
238 the specimens were left in room temperature in shade (22 to 29°C).

239 2.4. Testing

240 2.4.1. Flow properties

241 The flowability of fresh concrete was measured immediately after mixing using a standard flow table
242 test apparatus, in line with ASTM C1437 (ASTM C1437, 2020). As the copper slag is having least
243 percentage of absorbing water from the liquid used for mixing, it makes the concrete more viscous. The
244 flow test was conducted for the various mixes by varying dolomite content and percentage of steel fibers.

245

246 2.4.2. Compressive Strength

247 The typical Compression Testing Machine (CTM) with a 300-ton capacity is used to examine the
248 compressive strength of the concrete using cubes measuring 70.7 mm by 70.7 mm by 70.7 mm. The load
249 is applied at a rate of 5 kNs⁻¹ (1.0 MPas⁻¹) as suggested by ASTM 1856M-17 (ASTM C1856, 2017). The
250 tests were conducted after 1st, 3rd, 7th and 28th day of casting to analyze the effect of binder in early and
251 later strength.

252 2.4.3. Split Tensile strength

253 The tensile strength is an important parameter in developing Ultra-high performance in Geopolymer
254 Concrete. Due to the challenges of determining direct tensile strength through experimental methods, we
255 opted for the indirect approach of conducting Splitting tensile tests. These tests were performed on
256 cylindrical specimens measuring 100 mm diameter and 200 mm length in the standard CTM of 300 Ton
257 capacity. The cylinder is placed laterally and two metal strips were placed in the contact area of cylinder
258 the load is applied at the rate of 1.2 N/mm²/min in accordance with IS 5816(1999).

259 2.4.4. Flexural Strength

260 The assessment of flexural strength is experiment with prism specimens of size 100 mm x 100 mm x 400
261 mm. After 28-days curing the specimens were subjected to two-point loading in the UTM of 1000 kN
262 capacity. The loading rate maintained is from 1.6 to 1.8 kN/minute.

263 2.4.5. Water absorption and porosity

264 The water absorption of hardened concrete is due to capillary forces between the voids as in the soil
265 mass. The percentage of water absorption of the concrete sample measured will directly reflect the
266 volume of air pores and its network. The presence of air pores leads to entry of moisture in to the concrete
267 core resulting in corrosion of incorporated fibers and reinforcement. The water absorption is calculated
268 by the percentage of weigh of the cubes. The porosity is the measure of total percentage of volume of
269 voids compared to the specimen volume.

270 2.4.6. Micro properties

271 Microstructural properties of UHGPC samples with natural sand, copper slag, mix with optimal dolomite
272 content, and steel fiber composites were analyzed using a scanning electron microscope (SEM). The
273 SEM study was conducted using a third-generation TESCAN VEGA (LabIndia Instruments Pvt. Ltd,
274 Mumbai, India) scanning electron microscope, which has an acceleration voltage of 30 kV.

275 4. Results and Discussion

276 4.1. Flow properties of fresh concrete

277 The flow percentage of mixes used in both Phase-I and Phase-II of the experiment is tabulated in Table
278 5. The flowability of the mixes depends on the water absorption capacity of aggregates of liquid from
279 activating gel and reaction components of the precursors. Similarly, the steel fibers addition increased
280 the density of the fresh concrete. The addition of dolomite decreases the density of the mixes up to 30%
281 replacement of GGBS. The flow of various mixes was shown in Figure 5.

282 **Table 5.** Fresh density and flowability of mix

Mix	Fresh Density(kg/m ³)	Flow (%)
G100N100	2342.6	85
G100CS20	2416.2	86
G100CS40	2582.0	90
G100CS60	2636.2	91

G100CS80	2712.1	93
G100CS100	2752.1	100
G100D0SF0	2752.1	105
G100D0SF1	2767.0	104
G90D10SF0	2758.1	115
G90D10SF1	2793.8	111
G80D20SF0	2808.4	118
G80D20SF1	2823.8	112
G70D30SF0	2810.0	119
G70D30SF1	2833.6	117
G60D40SF0	2781.2	123
G60D40SF1	2809.3	120

283



284

285

a) b) c) d) e)

286

Figure 5. Flow of various UHPGC mixes a) G100N100 b) G100D0 c) G80D20SF0 d) G60D40SF0 e)

287

G80D20SF1

288

4.1.1. Effect of Copper slag

289

The copper slag, with its limited water absorption capacity, allows any excess water from the alkali liquid

290

to remain in the matrix (Ambily et al., 2015; Rajasekar, Arunachalam and Kottaisamy, 2019). This free water

291

makes the concrete more easily workable as the UHPGC needs nearly a self-compacting flowable mix.

292

The aggregates entrapped water increases as the copper slag quantity increases. Figure 5a and Figure 5b

293

shows the difference of flow between the UHPGC with natural aggregates and copper slag.

294

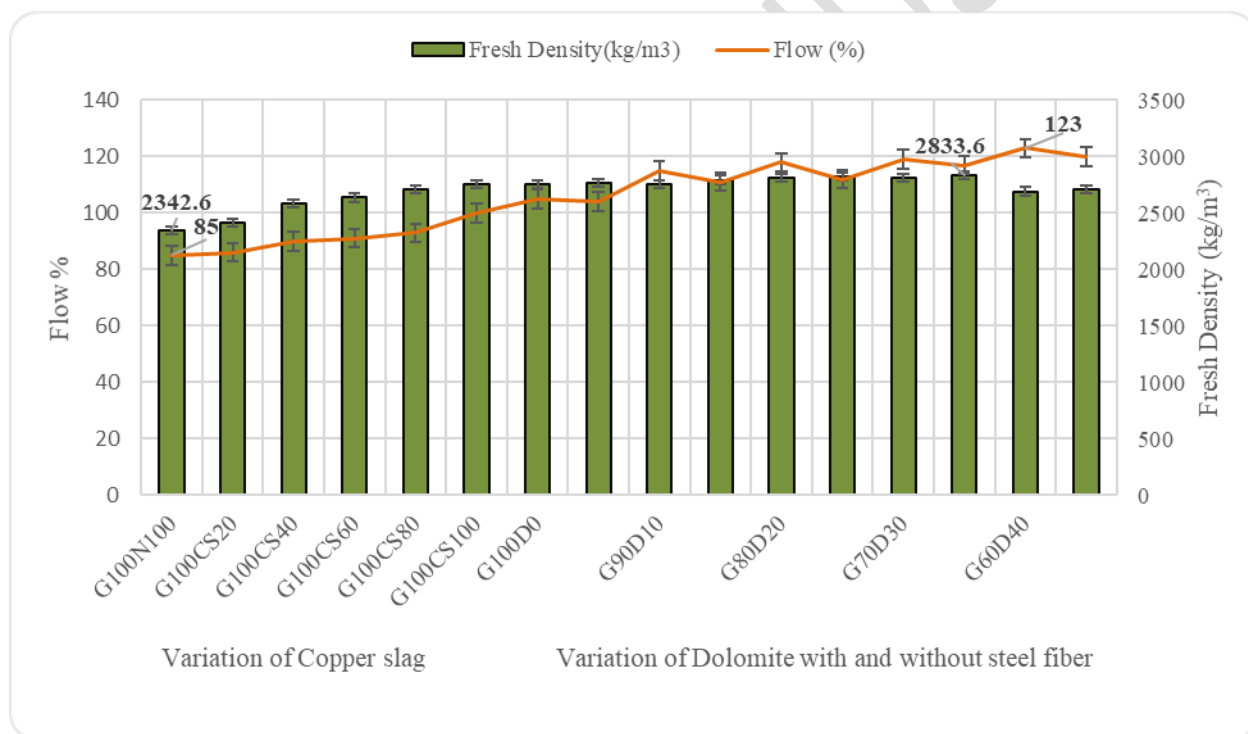
4.1.2. Effect of dolomite

295 The increase in dolomite content in the binder increased the flowability of the UHPGC. The workability
 296 of matrix where GGBS is the only precursor is very low compared to the matrix having 40% dolomite.
 297 The percentage of increase in flowability is nearly in 38% in the G60D40 matrix than G100D0 matrix.
 298 The fresh density is inversely proportional to the flowability as illustrated in Figure 6.

299 4.1.3. Effect of Steel fiber

300 In all the mixes irrespective of the aggregate and binder, the steel fiber addition decreased the flowability
 301 of the UHPGC.

302



303

304 **Figure 6.** Fresh density and Flow percentage of UHPGC

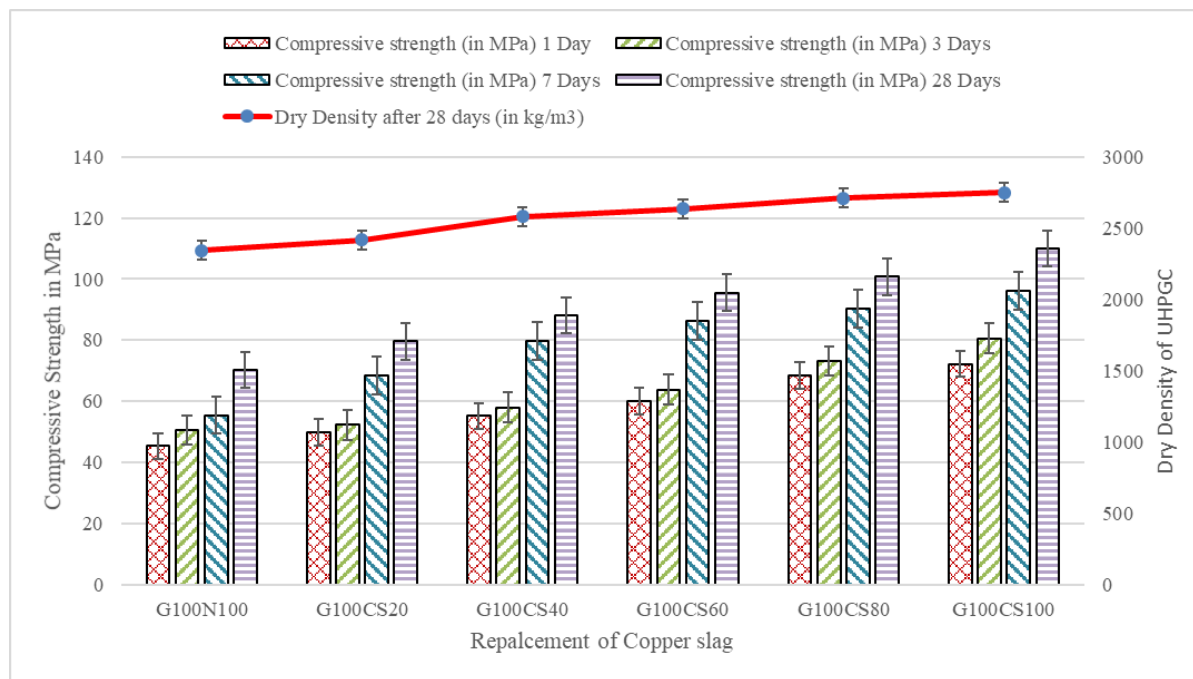
305 4.2 Compressive strength

306 4.2.1. Effect of copper slag

307 The compressive strength of the UHPGC were tabulated in Table 6. The compressive strength results
 308 from Phase-I of the experiment showed that the replacement of copper slag with natural aggregates
 309 improves the compressive strength. The copper slag addition increases the fresh and hard density of
 310 concrete. Its uneven form, jagged edges, and rough surface, in addition to its unit weight, enhance the
 311 bonding properties with the binder substance. From this initial study, it is evident that the copper slag
 312 can be effectively used as aggregate to achieve the high strength up to 110 MPa. The mixes having copper
 313 slag as aggregate is having 63.8% more compressive strength than the mix with M-Sand as aggregates.
 314 The GGBS based geopolymer matrix is known for its high early strength. For 100% copper slag based
 315 UHPGC, the 1-day strength, 3-day strength, 7-day strength are 65.6%, 73.2% and 87.4% of the 28-day
 316 strength which is very higher than conventional UHPC. It can be noted from the Figure 7, that the addition
 317 of copper slag does not influence the speed of strength attainment.

318 **Table 6.** Compressive strength of various UHPGC mixes

Mix	Dry Density after 28 days (in kg/m ³)	Compressive strength (in MPa)			
		1 Day	3 Days	7 Days	28 Days
G100N100	2342.6	45.3	50.6	55.5	70.2
G100CS20	2416.2	49.8	52.3	68.4	79.6
G100CS40	2582.0	55.2	58.0	79.7	88.2
G100CS60	2636.2	60.1	63.8	86.2	95.6
G100CS80	2712.1	68.5	73.2	90.4	100.8
G100CS100	2752.1	72.2	80.56	96.2	110.1
G100D0SF0	2752.1	72.2	80.56	96.2	110.1
G100D0SF1	2767.0	76.6	91.3	113.2	130.4
G90D10SF0	2758.1	64.0	73.2	102.0	115.8
G90D10SF1	2793.8	69.2	79.8	122.6	138.2
G80D20SF0	2808.4	63.9	77.6	106.8	119.2
G80D20SF1	2823.8	66.0	80.2	129.9	146.6
G70D30SF0	2810.0	52.6	66.8	106.0	114.6
G70D30SF1	2833.6	58.0	69.5	118.0	130.2
G60D40SF0	2781.2	45.3	55.2	90.2	105.0
G60D40SF1	2809.3	50.1	61.3	96.3	119.2



321

322 **Figure 7.** Dry density and Compressive Strength of UHPGC varying copper slag in fine aggregate

323 4.2.2. Effect of dolomite

324 Dolomite showed a superior performance in compressive strength up to 20% of replacement with GGBS.

325 The dolomite with 30% and 40% replacement showed a decreasing trend which is due to the presence of

326 magnesium ions. In previous observations, it has been established that magnesium ions can potentially

327 substitute a portion of the calcium ions in calcium silicate hydrate gels, or alternatively, create

328 magnesium silicate hydrate gels (Azimi et al., 2016). The effect of dolomite in compressive strength and

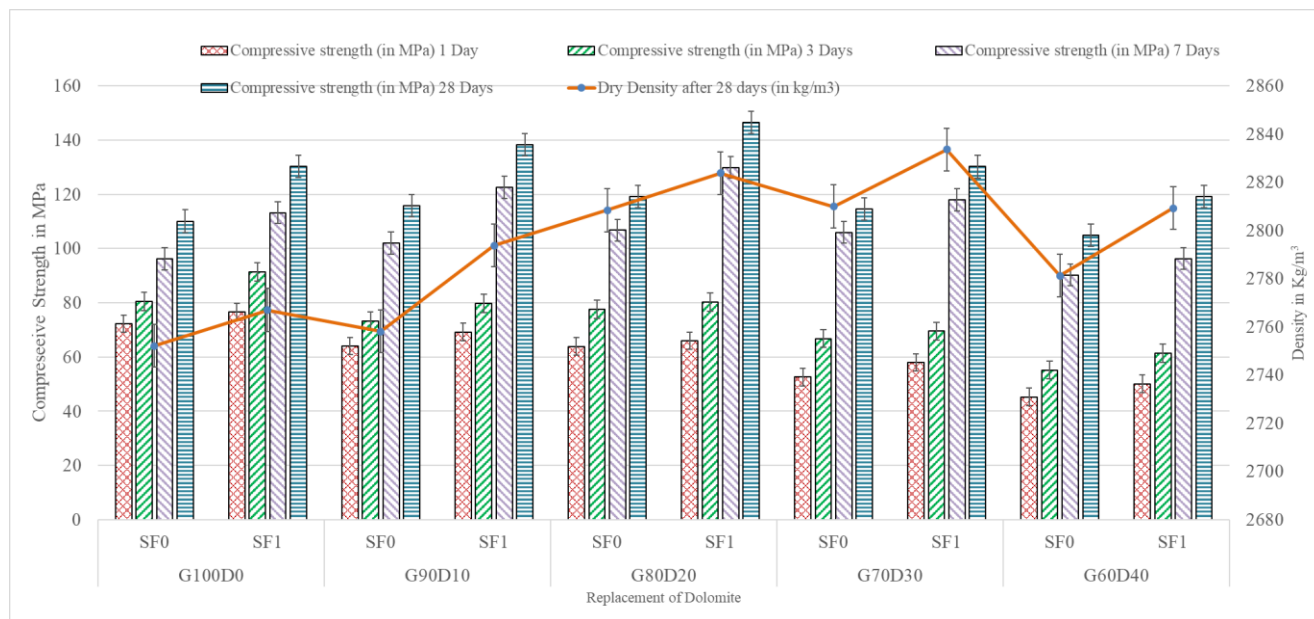
329 density is graphically illustrated in Figure 8. Adding dolomite makes the compression strength better

330 because it has a higher surface area to mass ratio than GGBFS. This makes the packing density higher,

331 which makes the strength higher. But when there is more dolomite (more than 20%), the $MgCO_3$ content

332 went up, which kept the gel from reacting. This made the UHPGPC mixes more uneven, which slowed

333 down the development of the compression strength values and made the microstructure partly weak.



335

336 **Figure 8.** Effect of dolomite in the compressive strength of UHPGC

337 From the Phase-I results, it was evident that the copper slag utilization up to 100% in fine aggregates
 338 gave best results compared to naturally occurring aggregates. Hence, the other mechanical properties like
 339 split tensile strength, flexural strength and physical properties like water absorption and porosity were
 340 experimented using copper slag as aggregates.

341 4.3. Splitting tensile strength

342 4.3.1. Effect of dolomite

343 Splitting tensile strength is an indirect way of determining the tensile strength of concrete. From Table
 344 7, it is evident that the split tensile strength of the UHPGC increases as the dolomite content increases.
 345 This may due to the higher reactivity of the calcium compounds and dense mix formation. The dense
 346 geopolymer gel creates a strong bond with granule of aggregates which makes a homogenous mix. On
 347 increasing the dolomite content over 20%, the unreactive compounds which acts as inert materials in
 348 forming CSH gel weaken the binding nature of the mix composition.

349 **Table 7.** Splitting Tensile strength and Flexural strength of UHPGC mixes

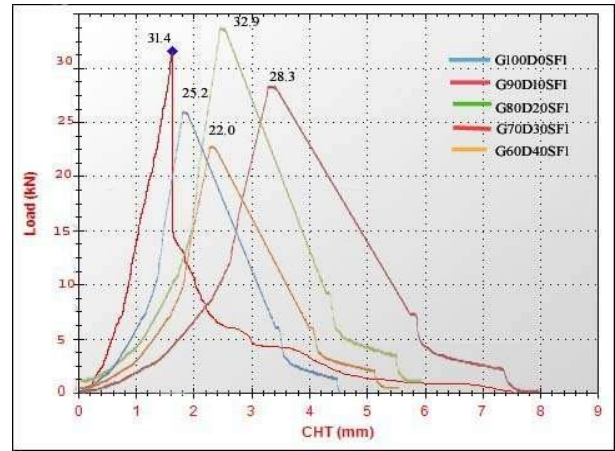
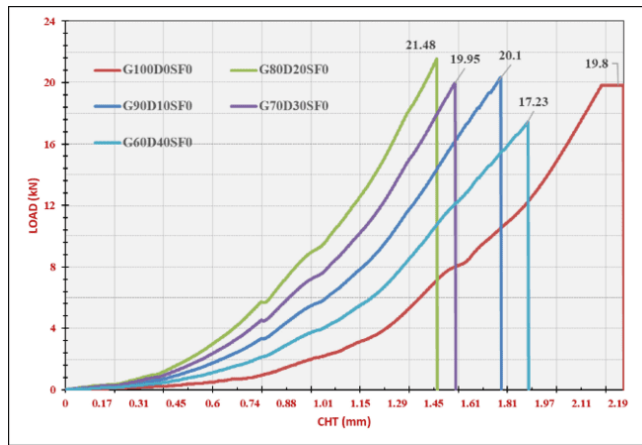
S.No.	Mix ID	Splitting Tensile strength (MPa)	Flexural strength (MPa)
1	G100D0SF0	8.15	9.9
2	G100D0SF1	9.49	12.6
3	G90D10SF0	8.54	10.05
4	G90D10SF1	11.21	14.15
5	G80D20SF0	9.20	10.74
6	G80D20SF1	12.36	16.45
7	G70D30SF0	9.36	9.98
8	G70D30SF1	11.85	15.7
9	G60D40SF0	8.95	8.62
10	G60D40SF1	10.19	11

350 4.3.2. Effect of steel fiber

351 The resistance to brittle failure of UHPGC was enhanced by the incorporation of steel fiber to attain
352 ultra-high strength in concrete (Guo and Yang, 2020). The split tensile strength is enhanced by the
353 incorporation of steel fiber, and the specimen is prevented from splitting by the crimped steel fibers. It
354 was clear that the UHPGC samples without fibers shows a brittle failure developed from a single crack,
355 whereas in UHPGC samples with steel fibers failed from multiple distributed cracks by proving the
356 enhancement of ductility to the concrete.

357 4.4. Flexural strength

358 The results of the tests conducted on the flexural strength of UHPGC with and without steel fibers
359 indicate that the presence of steel fiber significantly increases the post-crack straining of the material.
360 The flexural strength obtained from the maximum flexural load shows that the as the dolomite content
361 increases the flexural strength increases up to 20%. Then the strength decreases due to the high value of
362 unreacted calcium and magnesium content. The ultimate flexural load vs Cross Head Travel (CHT) of
363 the UHPGC with varying dolomite content is graphically illustrated in Figure 9a and 9b.



a)

(b)

Figure 9. a) Flexural load of the UHPGC without fibers (b) Flexural load of UHPGC with fiber

4.4.1. Effect of Steel fiber

The inclusion of steel fiber in UHPGC is intended to enhance its ductile property in bending. The UPGC is known for its brittle nature. It can be noted in Figure 9a and 9b that the post failure slope is gradually decreasing in the UHPGC specimen with steel fibers but there was a sudden brittle failure in specimen without fibers. The introduction of crimped steel fibers improves the concrete's ductile behavior, which in turn improves its flexural strength (Bhutta et al., 2017; Liu et al., 2020b; Lao et al., 2022). It is evident from the crack formation that specimen without fiber failed suddenly after first crack. But the UHPGC with fibers sustained the load through stretching of crimped fibers. The pattern of crack formed also is a non-linear crack showed the resistance developed against flexure.

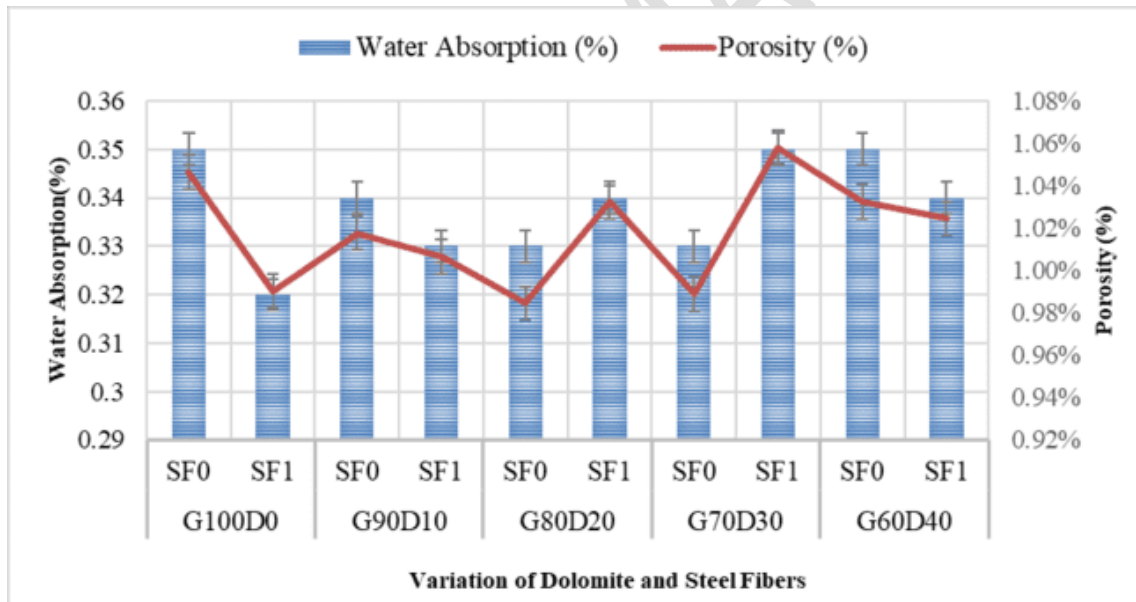
4.5. Water Absorption and Porosity

The samples were weighed before and after immersion in water. The percentages of water absorption and porosity are shown in Table 8. From Figure 10, it is evident that the water absorption and porosity increases as dolomite content increases up to 20%. Then the properties getting decreased on increasing the dolomite content. As a result of the high packing density and the substitution of GGBS with dolomite up to 20%, the intermolecular space was reduced significantly (Vaganov et al., 2017). But the increase of

382 dolomite increases the $MgCO_3$ content in the geopolymer matrix which leads to the inferior effects. The
 383 occurrence of white patches is observed in the cube specimens with 30% and 40% dolomite content. This
 384 may due to the unreacted $CaCO_3$ and $MgCO_3$ components.

385 **Table 8.** Water absorption and porosity of UHPGC

Sample ID	Water Absorption (%)	Porosity (%)
G100D0SF0	0.35	3.45
G100D0SF1	0.32	3.44
G90D10SF0	0.34	3.41
G90D10SF1	0.33	3.43
G80D20SF0	0.33	3.36
G80D20SF1	0.34	3.46
G70D30SF0	0.33	3.37
G70D30SF1	0.35	3.48
G60D40SF0	0.35	3.40
G60D40SF1	0.34	3.43

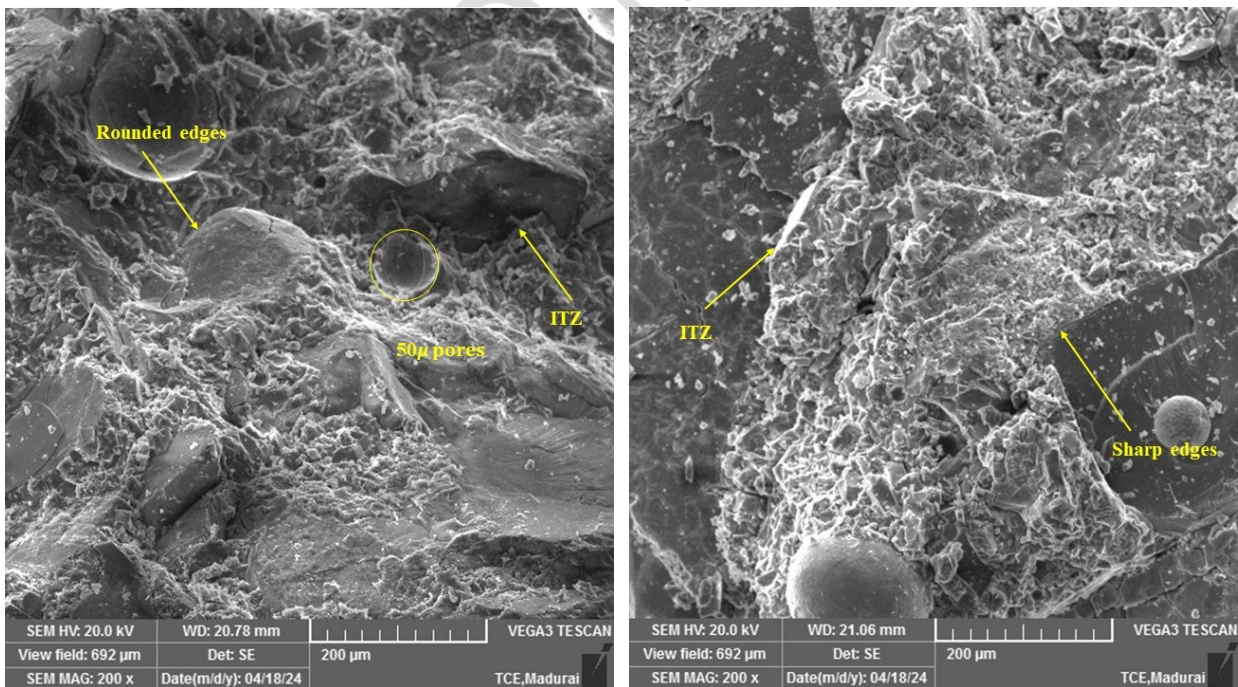


386

387 **Figure 10.** Water absorption and porosity of UHPGC Samples

388 4.6. Micro properties

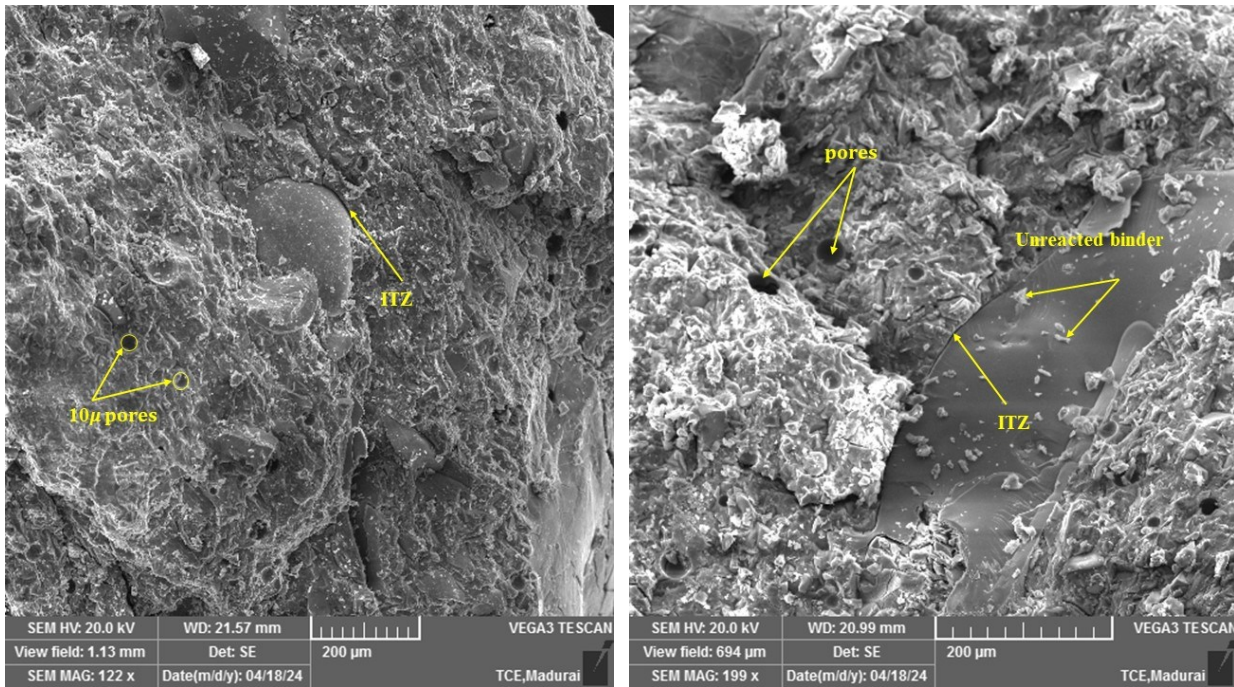
389 The microscopic images of UHPGC samples are presented in Figure 11 to 13. The fine aggregates under
 390 1.18mm used shows a good result in achieving high packing density. The influence of copper slag in
 391 UHPGC shows a huge impact in the bonding between binding gel and filler materials. In Figure 11a, it
 392 can be seen that the irregular rounded edges of natural aggregates create a smoother bond with the gel
 393 material, whereas from Figure 11b it is clear that the copper slag with its irregular sharp edges creates a
 394 stronger bond with gel materials. The multi-faceted granule with sharp edges bounds a strong
 395 adhesiveness towards the matrix. The Figure 16a and 16b are the micrographs of UHPGC with 20% and
 396 40% dolomite respectively. The former shows a strong bond compared to 100% GGBS matrix which is
 397 shown in Figure 11b. From the Figure 12b, it is evident that the white unreacted compounds created in
 398 the matrix is due to higher quantity of dolomite in binder. This forms a weaker matrix and more ITZ with
 399 aggregates. Similarly, from the Figure 13a and 13b, the matrix containing 40% dolomite form a weak
 400 bonding with fibers whereas the 20% dolomite gel forms a clear bonding with the fibers which reduces
 401 the network of weak zones enhancing higher compressive and tensile strength.



(a)

(b)

404 **Figure 11.** SEM images of UHPGC specimens with (a) natural aggregates and (b) Copper slag



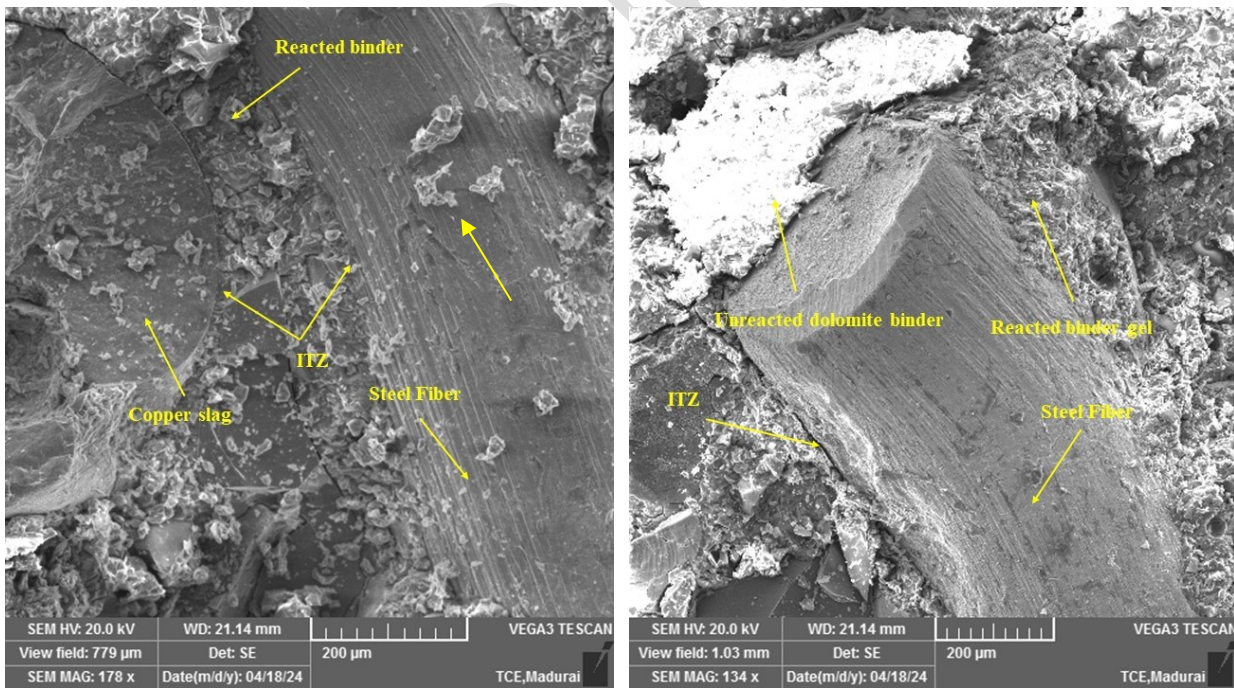
405

406

(a)

(b)

407 **Figure 12.** SEM images of UHPGC specimens with (a) 20% dolomite and (b) 40% dolomite



408

409

(a)

(b)

410 **Figure 13.** SEM images of fibers in UHPGC specimens with (a) 20% dolomite and (b) 40% dolomite

411 UHPGC with 20% dolomite exhibits a decrease in the occurrence of microvascular voids and micro
412 cracks. Microstructural studies indicated that the UHGPC made with GGBS-dolomite exhibited a denser
413 microstructure compared to the UHGPC made solely with GGBS.

414 **5. Conclusion**

415 The experimental findings clearly show that copper slag can be used as fine aggregate in UHPGC in
416 place of natural crushed aggregates. From this experimental study, following conclusions have been
417 made.

- 418 • The copper slag replacement can be made up to 100% in fine aggregate. The mixes having 100%
419 copper slag is having maximum flow of 17.65% than the mixes having natural aggregates. The
420 UHPGC samples with copper slag as fine aggregates is having 56.9% more compressive strength
421 than the samples having natural aggregates.
- 422 • As the dolomite content increases, the percentage of flowability increases. The mixes having 40%
423 dolomite replacement in GGBS is 23% more flowable than the mixes having 100% GGBS. As
424 the previous studies concluded, the addition of steel fiber decreases the flowability of the
425 UHPGC.
- 426 • When 20% of the dolomite content in the GGBS binder was substituted, the UHPGC mix showed
427 the highest compressive strength. Even though the main objective of adding dolomite is to
428 improve the workability, as an added advantage it improves the compressive strength up 20% of
429 replacement.
- 430 • Regarding indirect tensile and flexural properties, the optimum dolomite content in GGBS based
431 binder was found to be 20%. The increase in fresh and hardened density plays a vital role in the
432 superior mechanical behavior. Porosity and water absorption in the UHPGC reduced when
433 dolomite content raised up to 20% replacement in GGBS

434 • Microscopic tests show that replacing dolomite increased matrix-aggregate-steel fiber binding.
435 The ITZ of the 80%GGBS/20%Dolomite matrix bonds well, enhancing mechanical and
436 durability of the UHPGC composites. The study reveals that it is possible to produce the UHPC
437 with geopolymer technology by utilizing industrial by products as major ingredients. This study
438 has achieved a maximum compressive strength of 146.6 MPa and a maximum flexural strength
439 of 32.9 MPa.

440 The study's limitations arise from the use of copper slag as a fine substance, which is discharged as
441 land disposal in copper producing companies. The most difficult part of using copper slag is collecting
442 and sorting the material. The GGBS-based geopolymer composites have a quick setting characteristic,
443 requiring a fast casting process.

444 The results of this experimental investigation present good prospects for replacing natural sand with
445 copper slag and utilizing geopolymer technology to create UHPC. This could contribute to the production
446 of environmentally friendly building materials. This will create chances for the safe disposal of copper
447 slag and drastically reduce UHPC's excessive production costs. Because of its high specific gravity,
448 copper slag can be used in the high-performance concrete industry, which requires a larger consumption
449 of natural resources.

450 **Acknowledgments**

451 The authors express their gratitude to the Thiagarajar College of Engineering (TCE) for supporting us to
452 carry out this research work. Also, the financial support from TCE under Thiagarajar Research
453 Fellowship scheme (File.no: TRF/Jan-2023/14) is gratefully acknowledged.

454 **References**

- 455 Ahmed, A., Kumar, S.S. and Nanda, R.P. (2021), 'Development of geopolymer concrete mixes with ambient air
456 curing', IOP Conference Series: Materials Science and Engineering, 1116(1), 012160.
- 457 Amar, R., Devanand, R., Harsha, H.N. and Sachin, K.C. (2023), 'Experimental studies on GGBS based
458 geopolymer concrete', Materials Today: Proceedings [Preprint].

- 459 Ambily, P.S., Ravisankar, K., Umarani, C., Dattatreya, J.K. and Iyer, N.R. (2014), 'Development of ultra-high-
460 performance geopolymer concrete', *Magazine of Concrete Research*, 66(2), 82–89.
- 461 Ambily, P.S., Umarani, C., Ravisankar, K., Prem, P.R., Bharkumar, B.H. and Iyer, N.R. (2015), 'Studies on ultra
462 high performance concrete incorporating copper slag as fine aggregate', *Construction and Building Materials*, 77,
463 233–240.
- 464 Ansari, N. and Bandewar, D.K. (2022), 'Experimental Study of the Physical Properties of Concrete Prepared by
465 Partial Replacement of Cement with Alccofine, Metakaolite and GGBS', *International Journal for Research in
466 Applied Science and Engineering Technology*, 10(8), 1344–1362.
- 467 Azimi, E.A., Abdullah, M.M.A.B., Vizureanu, P., Salleh, M.A.A.M., Sandu, A.V., Chaiprapa, J., Yoriya, S.,
468 Hussin, K. and Aziz, I.H. (2020), 'Strength development and elemental distribution of dolomite/fly ash
469 geopolymer composite under elevated temperature', *Materials*, 13(4).
- 470 Azimi, E.A., Abdullah, M.M.A.B., Ming, L.Y., Yong, H.C., Hussin, K. and Aziz, I.H. (2016), 'Review of
471 Dolomite as Precursor of Geopolymer Materials'. *MATEC Web of Conferences* 78(18):01090.
- 472 Bhutta, A., Borges, P.H.R., Zanotti, C., Farooq, M. and Banthia, N. (2017), 'Flexural behavior of geopolymer
473 composites reinforced with steel and polypropylene macro fibers', *Cement and Concrete Composites*, 80, 31–40.
- 474 Brindha, D. and Nagan, S. (2011), *Durability Studies on Copper Slag Admixed Concrete*, *Asian Journal Of Civil
475 Engineering (Building And Housing)*. Available at: www.SID.ir.
- 476 Chithambar Ganesh, A., Siva Kumar, P., Kapilan, S., Kumar, A., Nazeer Basha, S. and Tejaeswar, V. (2023),
477 'Effect of alkaline activator solution over GGBS based concrete under ambient curing', *Materials Today:
478 Proceedings [Preprint]*.
- 479 Davidovits, J. (1991), 'Geopolymers - Inorganic polymeric new materials', *Journal of Thermal Analysis*, 37(8),
480 1633–1656.
- 481 Davidovits J (1988): *Proceedings Geopolymer'88(1988)*, Available at:
482 https://scholar.google.com/scholar_lookup?title=Proceedings+Geopolymer&author=Davidovits,+J.&author=Orlinski,+J.&publication_year=1988 (Accessed: 3 May 2024).
- 483
- 484 Dineshkumar, M. and Umarani, C. (2020), 'Effect of Alkali Activator on the Standard Consistency and Setting
485 Times of Fly Ash and GGBS-Based Sustainable Geopolymer Pastes', *Advances in Civil Engineering*, 2020.
- 486 Ding, Y., Shi, C.J. and Li, N. (2018), 'Fracture properties of slag/fly ash-based geopolymer concrete cured in
487 ambient temperature', *Construction and Building Materials*, 190, 787–795.
- 488 Divekar, R.S. and Sawant, R.M. (2023), 'Dolomite Powder in Concrete: A Review of Mechanical Properties and
489 Microstructural Characterization', *Civil Engineering and Architecture*, 11(6), 3314–3321.
- 490 Rameshwaran, P.M. & Madhavi, T.. (2021), 'Flexural behaviour of fly ash based geopolymer concrete', *Materials
491 Today: Proceedings*. 46. 10.1016/j.matpr.2020.11.755.
- 492 Goldsmith, J.R. and Graf, D.L. (1958), 'Structural and Compositional Variations in Some Natural Dolomites',
493 <https://doi.org/10.1086/626547>, 66(6), 678–693.

494 Guo, X. and Yang, J. (2020), 'Intrinsic properties and micro-crack characteristics of ultra-high toughness fly
495 ash/steel slag based geopolymer', *Construction and Building Materials*, 230, 116965.

496 Gusain, I., Sharma, S., Debarma, S., Kumar Sharma, A., Mishra, N. and Prakashrao Dahale, P. (2023), 'Study of
497 concrete mix by adding Dolomite in conventional concrete as partial replacement with cement', *Materials Today:
498 Proceedings*, 73, 163–166.

499 Habert, G., Denarié, E., Šajna, A. and Rossi, P. (2013), 'Lowering the global warming impact of bridge
500 rehabilitations by using Ultra High Performance Fibre Reinforced Concretes', *Cement and Concrete Composites*,
501 38, 1–11.

502 Hardjito, D., Wallah, S.E., Sumajouw, D.M.J. and Rangan, B. V (2005), 'Fly Ash-Based Geopolymer Concrete',
503 *Australian Journal of Structural Engineering*, 80(1), 20–24.

504 Hu, H., Yao, W. and Wei, Y. (2023), 'Recycling waste dolomite powder in cement paste: Early hydration process,
505 microscale characteristics, and life-cycle assessment', *Science of The Total Environment*, 902, 166008.

506 'IS-16714 (2018), 'Ground Granulated Blast Furnace Slag for Use in Cement, Mortar and Concrete-
507 Specification', Bureau of Indian Standards.

508 Huixia Wu, Cheng Liu, Yasong Zhao, Gaofeng Chen, Jianming Gao(2024), 'Elucidating the role of recycled
509 concrete powder in low-carbon ultra-high performance concrete (UHPC): Multi-performance evaluation',
510 *Construction and Building Materials*,441.

511 Huixia Wu, Xin Liu, Changqing Wang, Youchao Zhang, Zhiming Ma(2024), 'Micro-properties and mechanical
512 behavior of high-ductility engineered geopolymer composites (EGC) with recycled concrete and paste powder as
513 green precursor', *Cement and Concrete Composites*, 152.

514 Huixia Wu, Jianming Gao, Cheng Liu, Zhaoheng Guo, Xu Luo(2024), 'Reusing waste clay brick powder for low-
515 carbon cement concrete and alkali-activated concrete: A critical review', *Journal of Cleaner Production*,449.

516 Kathirvel, P. and Sreekumaran, S. (2021), 'Sustainable development of ultra-high-performance concrete using
517 geopolymer technology', *Journal of Building Engineering*, 39.

518 Kavitha, S. and Felix Kala, T. (2016), 'Evaluation of strength behavior of self-compacting concrete using alccofine
519 and GGBS as partial replacement of cement', *Indian Journal of Science and Technology*, 9(22).

520 Kisan, M. and Sangathan, S. (1970), 'Specification for Coarse and Fine Aggregates from Natural Sources for
521 Concrete [CED 2: Cement and Concrete]', IS, 383.

522 Lao, J.C., Xu, L.Y., Huang, B.T., Dai, J.G. and Shah, S.P. (2022), 'Strain-hardening Ultra-High-Performance
523 Geopolymer Concrete (UHPC): Matrix design and effect of steel fibers', *Composites Communications*, 30,
524 101081.

525 Liu, Y., Zhang, Z., Shi, C., Zhu, D., Li, N. and Deng, Y. (2020a), 'Development of ultra-high performance
526 geopolymer concrete (UHPC): Influence of steel fiber on mechanical properties', *Cement and Concrete
527 Composites*, 112.

528 Liu, Y., Zhang, Z., Shi, C., Zhu, D., Li, N. and Deng, Y. (2020b), 'Development of ultra-high performance
529 geopolymer concrete (UHPC): Influence of steel fiber on mechanical properties', *Cement and Concrete
530 Composites*, 112.

531 Iyu, B., Wang, A., Zhang, Z., Liu, K., Xu, H., Shi, L. and Sun, D. (2019), 'Coral aggregate concrete: Numerical
532 description of physical, chemical and morphological properties of coral aggregate', *Cement and Concrete*
533 *Composites*, 100, 25–34.

534 De Oliveira, L.B., de Azevedo, A.R.G., Marvila, M.T., Pereira, E.C., Fediuk, R. and Vieira, C.M.F. (2022),
535 'Durability of geopolymers with industrial waste', *Case Studies in Construction Materials*, 16.

536 Panagiotopoulou, C., Kontori, E., Perraki, T. and Kakali, G. (2007), 'Dissolution of aluminosilicate minerals and
537 by-products in alkaline media', *Journal of Materials Science*, 42(9), 2967–2973.

538 Patil, S. V., Karikatti, V.B. and Chitawadagi, M. (2018), 'Granulated Blast-Furnace Slag (GGBS) based
539 Geopolymer concrete - Review Concrete - Review', *International Journal of Advanced Science and Engineering*,
540 5(1), 879.

541 Rajasekar, A., Arunachalam, K. and Kottaisamy, M. (2018), 'Durability of ultra high strength concrete with Waste
542 Granite Sand as partial substitute for aggregate', *Journal of Computational and Theoretical Nanoscience*, 15(2),
543 446–452.

544 Rajasekar, A., Arunachalam, K. and Kottaisamy, M. (2019), 'Assessment of strength and durability characteristics
545 of copper slag incorporated ultra high strength concrete', *Journal of Cleaner Production*, 208, 402–414.

546 R, B. and J, S. (2019), 'Effect of Alccofine and GGBS Addition on the Durability of Concrete', *Civil Engineering*
547 *Journal*, 5(6), 1273–1288.

548 Saranya, P., Nagarajan, P. and Shashikala, A.P. (2019), 'Development of ground-granulated blast-furnace slag-
549 dolomite geopolymer concrete', *ACI Materials Journal*, 116(6), 235–243.

550 Saranya, P., Nagarajan, P. and Shashikala, A.P. (2020), 'Impact Resistance of GGBS-Dolomite Geopolymer
551 Concrete', in *IOP Conference Series: Materials Science and Engineering*. IOP Publishing Ltd.

552 Sharma, A.K. and Sivapullaiah, P. V. (2016), 'Ground granulated blast furnace slag amended fly ash as an
553 expansive soil stabilizer', *Soils and Foundations*, 56(2), 205–212.

554 Shi, C., Meyer, C. and Behnood, A. (2008), 'Utilization of copper slag in cement and concrete', *Resources*,
555 *Conservation and Recycling*, 1115–1120.

556 Singh, B., Ishwarya, G., Gupta, M. and Bhattacharyya, S.K. (2015), 'Geopolymer concrete: A review of some
557 recent developments', *Construction and Building Materials*, 85, 78–90.

558 Sontakki, M.S. and Cholekar, S.B. (2015), 'Strength Performance Studies on Ambient Cured Silica fume based
559 Geopolymer Concrete', *International Research Journal of Engineering and Technology [Preprint]*. Available at:
560 www.irjet.net.

561 ASTM C 1856(2017), 'Standard Practice for Fabricating and Testing Specimens of Ultra-High-Performance
562 Concrete 1', ASTM International.

563 ASTM C 1437 (2020), 'Standard Test Method for Flow of Hydraulic Cement Mortar 1', ASTM International.

564 UNSTATS. Greenhouse gas emissions by sector (absolute... - Google Scholar (no date),. Available at:
565 [https://scholar.google.com/scholar?q=UNSTATS.%20Greenhouse%20gas%20emissions%20by%20sector%20\(a](https://scholar.google.com/scholar?q=UNSTATS.%20Greenhouse%20gas%20emissions%20by%20sector%20(a)

566 absolute%20values).%20United%20Nation%20Statistical%20Division%3A%20Springer%3B%202010.
567 (Accessed: 2 May 2024).

568 Vaganov, V., Kireev, A., Avdeev, S., Šahmenko, G. and Šinka, M. (2017), 'Prospects for Effective Use of
569 Dolomite in Concrete Compositions', *Construction Science*, 19(1).

570 Vinotha Jenifer, J., Brindha, D., Annie Sweetlin Jebarani, J.P., Venkadapriya, S. and Pandieswari, M. (2023),
571 'Mechanical and microstructure properties of copper slag-based basalt fiber reinforced concrete', *Materials Today:*
572 *Proceedings [Preprint]*.

573 Wang, X.-H., Val, D. V, Zheng, L. and Roderick Jones, M. (2017), 'Influence of loading and cracks on carbonation
574 of RC elements made of different concrete types', *Construction and Building Materials*, 164, 12–28.

575 Wang, Y., Shui, Z., Gao, X., Huang, Y., Yu, R., Li, X. and Yang, R. (2019), 'Utilizing coral waste and metakaolin
576 to produce eco-friendly marine mortar: Hydration, mechanical properties and durability', *Journal of Cleaner*
577 *Production*, 219, 763–774.

578 Wan, X., Shen, C., Wang, P., Zhao, T. and Lu, Y. (2020), 'A study on fracture toughness of ultra-high toughness
579 geopolymer composites based on Double-K Criterion', *Construction and Building Materials*, 251.

580 Wetzel, A. and Middendorf, B. (2019), 'Influence of silica fume on properties of fresh and hardened ultra-high-
581 performance concrete based on alkali-activated slag', *Cement and Concrete Composites*, 100, 53–59.

582 Wong, L.S. (2022), 'Durability Performance of Geopolymer Concrete: A Review', *Polymers*. MDPI.

583 Wu, H., Gao, J., Liu, C., Guo, Z. and Luo, X. (2024), 'Reusing waste clay brick powder for low-carbon cement
584 concrete and alkali-activated concrete: A critical review', *Journal of Cleaner Production*, 449, 141755.

585 Yoo, D.Y., Banthia, N., Kang, S.T. and Yoon, Y.S. (2016), 'Size effect in ultra-high-performance concrete beams',
586 *Engineering Fracture Mechanics*, 157, 86–106.

587 Yunsheng, Z. and Wei, S. (2006), 'Fly ash based geopolymer concrete', *Indian Concrete Journal*, 80(1), 20–24.

588